Integrated geophysical application to investigate groundwater potentiality of the shallow Nubian aquifer at northern Kharga, Western Desert, Egypt

Abdellatif Younis [a],[*], Mamdouh Soliman [a], Salah Moussa [b], Usama Massoud [a], Sami Abd ElNabi [b], Magdy Attia [a]

[a] National Research Institute of Astronomy and Geophysics, NRIAG, 11421 Helwan, Cairo, Egypt
[b] Geophysics Department, Faculty of Science, Ain Shams University, Abbasia, Cairo, Egypt

Abstract Continuous evaluation of groundwater aquifers in the basin of Kharga Oasis is very important. Groundwater in Kharga Oasis represents the major factor for the development plans of this area as it is the sole source for water supplies required for drinking and irrigation purposes. This study is concerned by analyzing the groundwater potentiality of the shallow aquifer at the northern part of Kharga basin by integrated application of Vertical Electrical Sounding (VES) and Time domain Electromagnetic (TEM) techniques. The VES data were measured at 28 points arranged along a north–south trending line by applying Schlumberger array with a maximum current-electrode spacing (AB) of 1000 m. The TEM data were measured at 167 points arranged along 11 east–west trending lines by using a single square loop with 50 m loop-side length. The VES and TEM data have been individually inverted, where the VES models were used as initial models for TEM data inversion. The final models were used for construction of 17 geoelectrical sections and 5 contour maps describing subsurface water-bearing layers at the investigated area. Correlation of the obtained models with geologic, hydrogeologic and borehole information indicates that the shallow aquifer comprises two zones (A-up) and (B-down) separated by a highly conductive shale layer. The upper zone (A) is composed of fine to medium sand with thin clay intercalations. It exhibits low to moderate resistivities. This zone was detected at depth values ranging from 10 to 70 m below ground surface (bgs) and shows a thickness of 25–90 m. The lower zone (B) exhibits moderate to high resistivity values with expected good water quality. The upper surface of zone B was detected at 60–165 m depth.
© 2016 Production and hosting by Elsevier B.V. on behalf of National Research Institute of Astronomy and Geophysics. This is an open access article under the CC BY-NC-ND license (http://creativecommons.org/licenses/by-nc-nd/4.0/).

* Corresponding author.
 E-mail address: abdougeoman@yahoo.com (A. Younis).

1. Introduction

Kharga city, the capital of Al-Wadi Al-Gadid governorate is located at 140 km east of Dakhla Oasis and 220 km south of Assiut city. It is bounded by longitudes 30°20′ and 30°40′E and latitudes 25°05′ and 25°30′N (CONOCO, 1987). It is bounded by the Eocene limestone plateau from the east to north. This limestone plateau stretches along Middle and Upper Egypt with an elevation of up to 550 m above the sea level (El-Sankary, 2002).

Kharga Oasis depends on groundwater as the sole source for water supplies. It is suffering from continuous lowering in groundwater level due to the excessive and unplanned groundwater withdrawal. So it is necessary to study the aquifer of Kharga Oasis continuously to define the areal extension of water-bearing zones (Soliman, 2013).

Geophysical investigations play an important role for groundwater evaluation, as it may offer a means of addressing groundwater potentiality, by providing a spatially extensive, non-invasive means of investigating the subsurface. In the past, applications of geophysical methods in groundwater and vadose zone hydrology have mainly focused on mapping geological structures (e.g. clay/sand layers, bedrock valleys), delineation of aquifer boundaries, mapping of fracture zones, etc. In summary, the focus has been directed for a long time on the "geometrical" characterization of the subsurface. For such purposes standard methods are presently available and well-documented in the literature. Recently, increased attention has been given to the use of geophysical methods to derive parameters and state variables characterizing especially near surface groundwater systems and soils (Vereecken et al., 2002, 2004; Rubin and Hubbard, 2005). Classical approaches such as drilling and coring have shown their limitations in capturing this spatial and temporal variability. Characterizing spatial and temporal variability of aquifers is, however, a key factor determining e.g. success of water management strategies or predicting pollution risks to water supply systems.
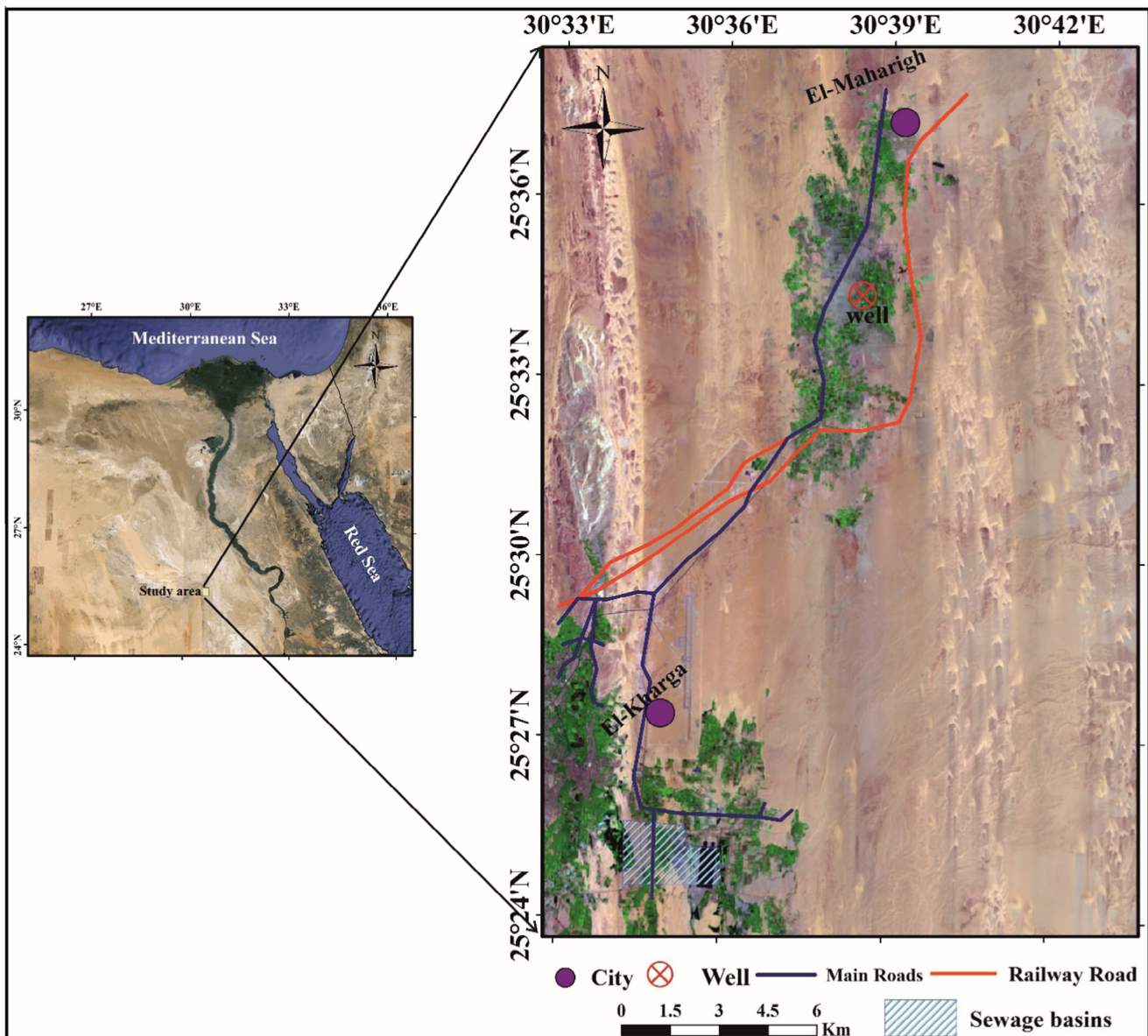
Figure 1   Enhanced Thematic Mapper (ETM) landsat image showing location of the study area.
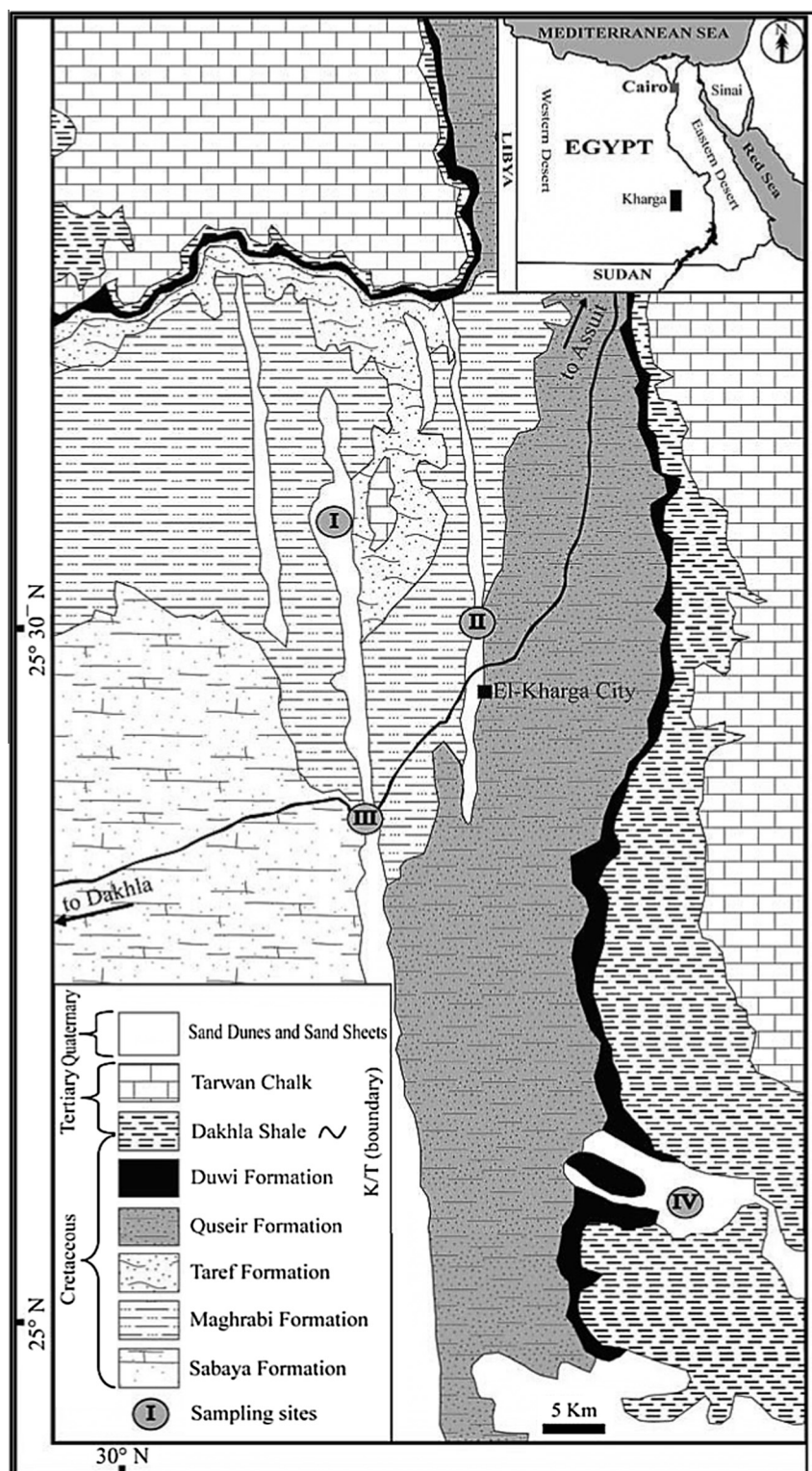
Figure 2 Geological map of the study area (after CONOCO, 1987 and Abu Seif 2013).

The present study aims to evaluate the conditions of groundwater occurrences and their extension by an integrated application of electric and electromagnetic techniques. The studied area covers about 410 km^2 and occupies the northern part of Kharga basin. It is bounded by longitudes 30°33′, 30°43′12″E and latitudes 25°37′48″, 25°25′12″N (Fig. 1).

2. Geological setting

The geology of Western Desert, including Kharga Oasis, is very well documented in Knetsch and Yallouze (1955), Said (1962, 1990), Issawi and El-Hinnawi (1982), Salman (1984), Salman et al. (1984) and El-Hinnawi et al. (2005). From the
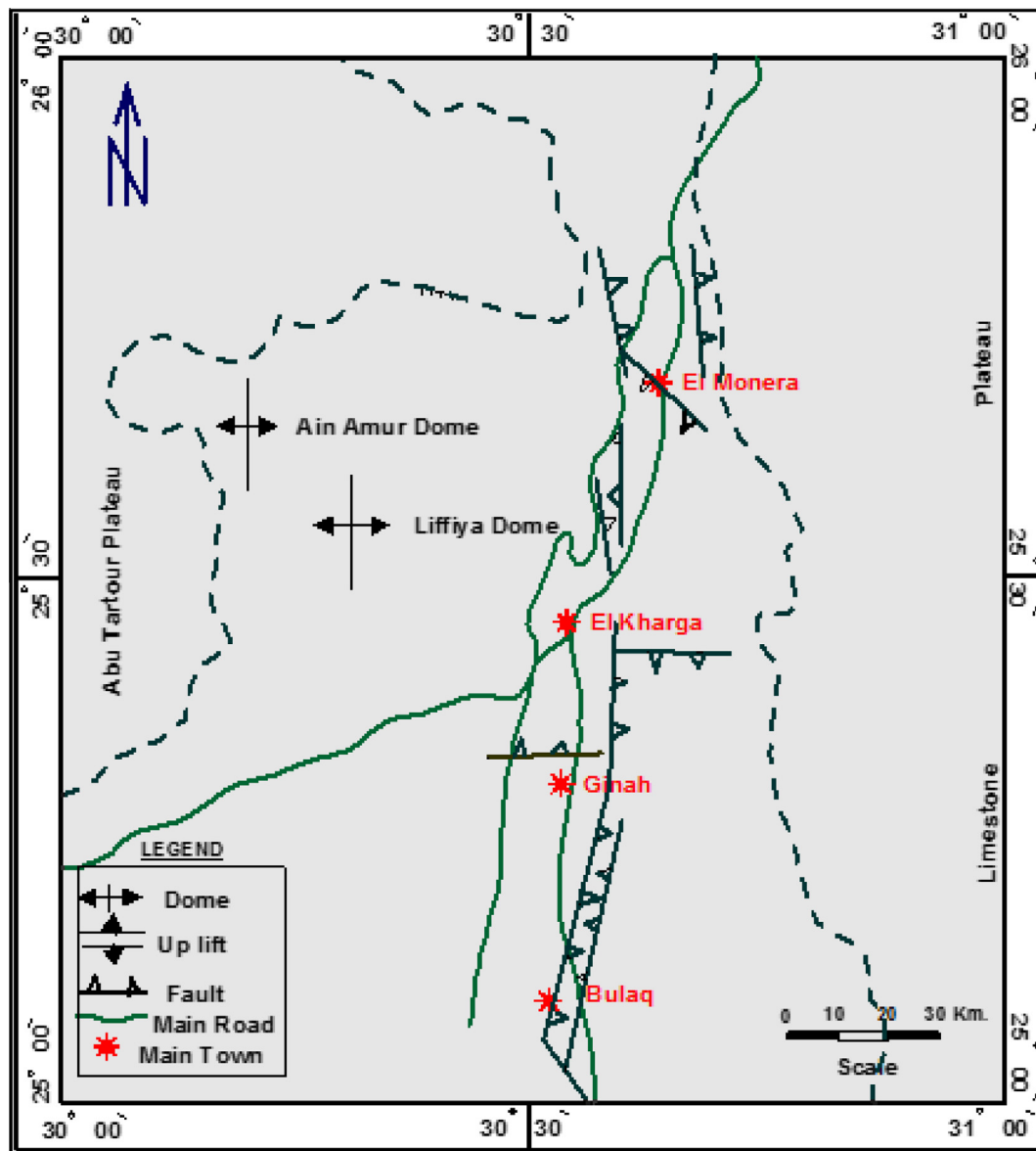
Figure 3 General structure map of northern Kharga (Shata, 1961).

geological point of view, the Lower Cretaceous-Lower Tertiary sedimentary sequence overlies unconformably the Precambrian basement rocks at Kharga basin. This sedimentary sequence comprises the Nubian sandstone overlain by variegated shale rock units, which are well exposed forming most bedrocks of the depression floor. These widely exposed rock units are followed upward by the Duwi, Dakhla, Tarawan, Esna and Thebes formations exposed on the eastern and the northern scarps bounding the depression. Furthermore, the Quaternary times in the study area were characterized by alternating periods of wet and dry climates, which resulted in several fluvial, lacustrine and aeolian deposits strewn on the depression floor (Beadnell, 1933; El-Sankary, 2002; Salman et al., 2010).

Geomorphologically, the area is covered mostly by blown and unblown sand and lake deposits, where the latter is being altered in fertile land in the process of agricultural development as shown in Fig. 2.

Many authors such as Shata (1961), Ezzat and Abou El-Atta (1974) and El-Shazly et al. (1959) studied the subsurface geology of Kharga Oasis based on the drilling results of nine wells. They estimated the total maximum thickness of the Nubian succession at about 1400 m. Ezzat and Abou El-Atta (1974) identified the water-bearing zones in the Nubian series, and indicated that the Nubian sandstone of Cretaceous age constitutes the main rock unit in the subsurface in the study area. The Nubia facies are composed of sandstone, siltstone interbedded with shale and occasional conglomerates. It rests unconformably on the Precambrian rocks at different depths due to the effect of structural elements Abdallah (2000).

Structurally, Shata (1961) assumed that both Kharga and Dakhla depressions (Fig. 3) represent two structurally low areas (down folds) occurring on both sides of a major structural high (up fold). Ghobrial (1967) identified two tectonic movements which affected the area; the first is a Pre-Maestrichtian movement which caused the formation of
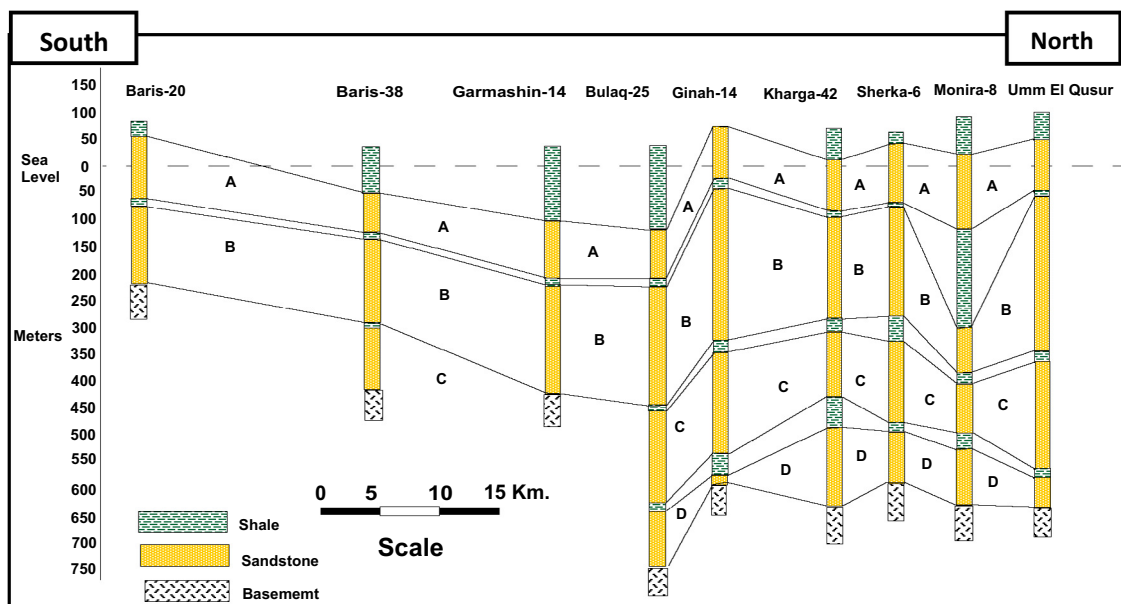
Figure 4 North–south hydrogeologic cross section passing through the study area (Modified after Abd Allah, 2013).
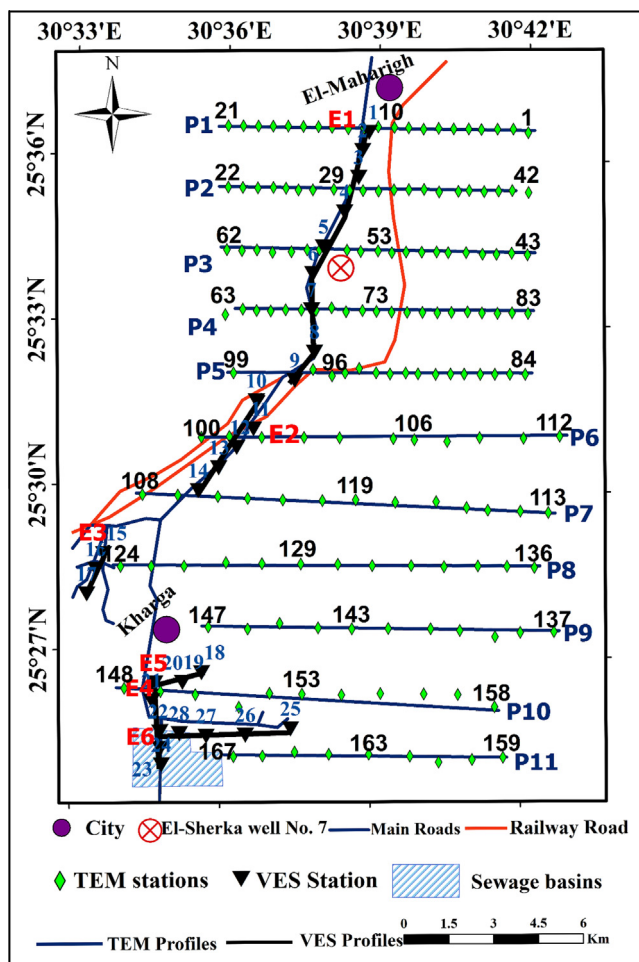

Figure 5 Location map of VES/TEM data points and geoelectrical cross sections.

Kharga and Baris depositional basins and the second is the development of an older joint system which characterized the Nubian Formation in Kharga Oasis.

3. Hydrogeologic setting

The Nubian facies constitutes the main groundwater aquifer in the study area. It consists of alternating beds of clay, shale, sand and sandstone. Nubian sandstone aquifer is divided into four zones (Fig. 4) termed from top to bottom as A, B, C and D (Diab, 1978; RIGW, 2006; and Abd Allah, 2013). The uppermost zone (A) is composed of fine to very coarse sandstone intercalated with shale beds. Some parts are completely formed of gravel and constituents of limonite, muscovite, pyrite and glauconitic are frequently present (Fig. 4).

Zone B is composed of fine to coarse sandstone intercalated with shale beds. Shale is multicolored, moderately hard, grey, green, brown and yellow due to staining with iron oxides. Zone C is composed of sandstone mostly subangular to subround and shale, mostly brown, red, grey green and fissile. Zone D is the lowest zone in the Nubian sandstone formation. It rests unconformably on the basement complex. This zone is mainly formed of sandstone, mostly white, pale yellow and pale red, very coarse to coarse, with little gravels.

4. Data acquisition

The VES data were measured in the study area at 28 measuring points aligned along Kharga–Assiut road and some crossing roads. Resistivity data have been acquired by using Syscal R2 resistivity meter, where the standard Schlumberger electrode configuration with AB spacing varying logarithmically from 2 m to 1000 m was applied. For reliability, the VES No. 6 was taken close to El-Sherka well No. 7 where some information (e.g. well depth, depth of water, screen depth, water quality) was available.
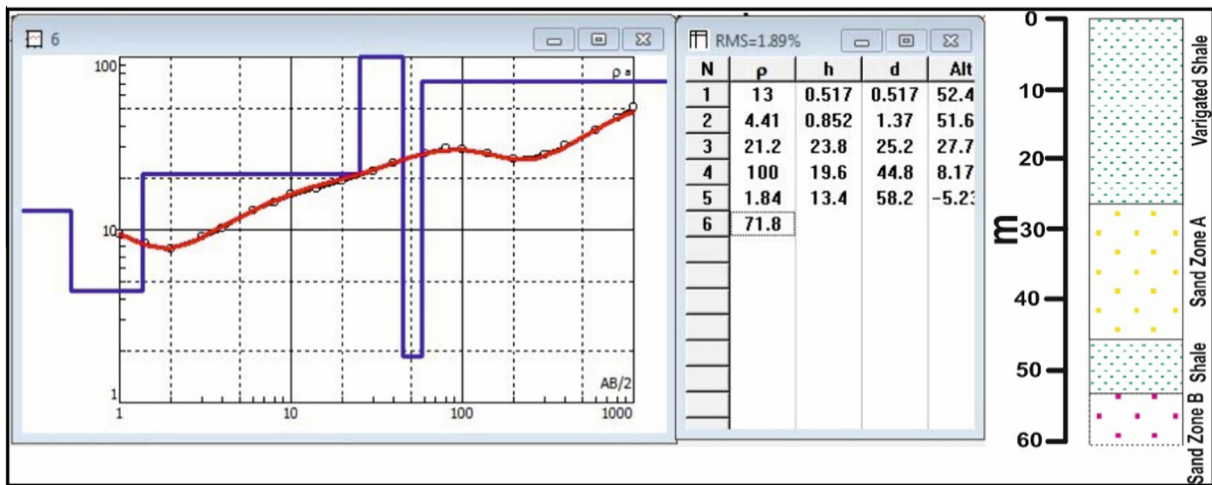
Figure 6 1-D model obtained from VES data inversion at sounding point No. 6 correlated with borehole information El-Sherka well No. 7.
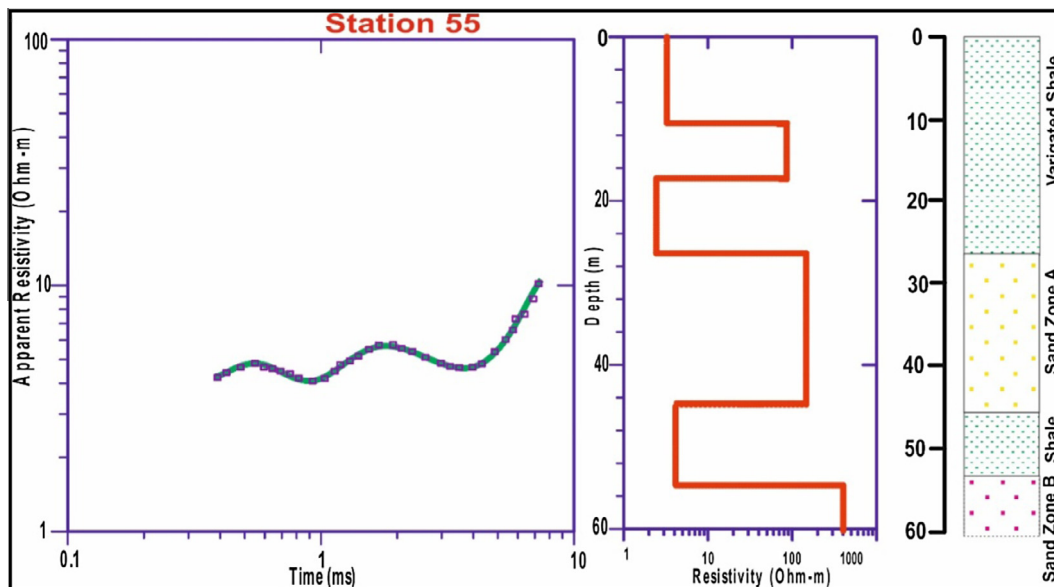

Figure 7 1-D model obtained from TEM data inversion at point No. 55 correlated with borehole lithologic units of El-Sherka well No. 7.

Figure 8 Geoelectrical/geological cross section constructed from VES models along profile E1.

Figure 9   Geoelectrical/geological cross section constructed from VES models along profile E3.

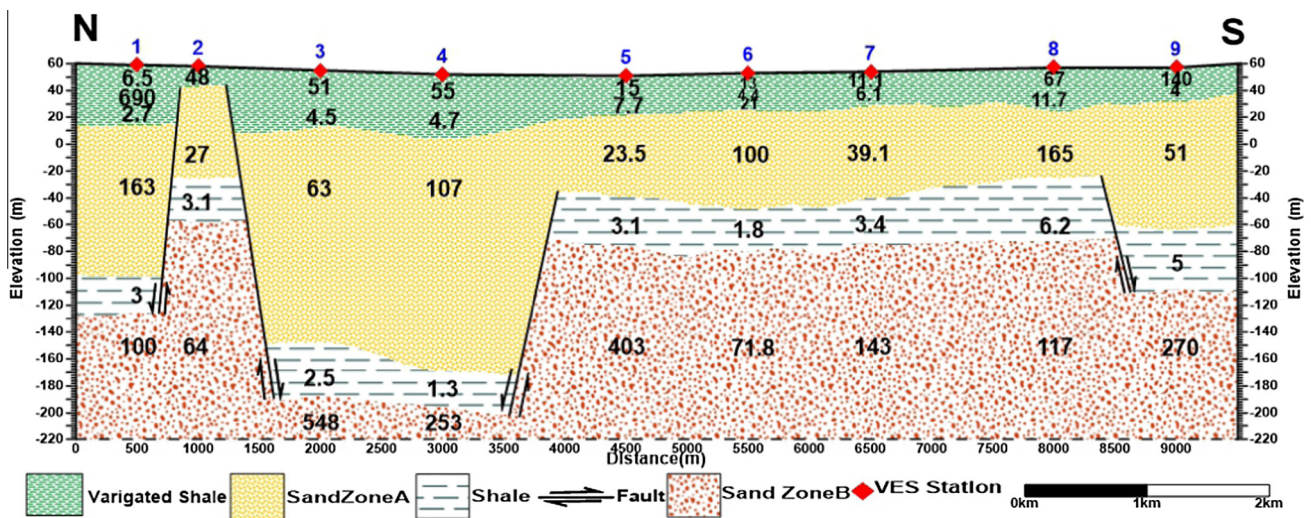**Figure 10**   Geoelectrical/geological cross section constructed from TEM models along profile P1.
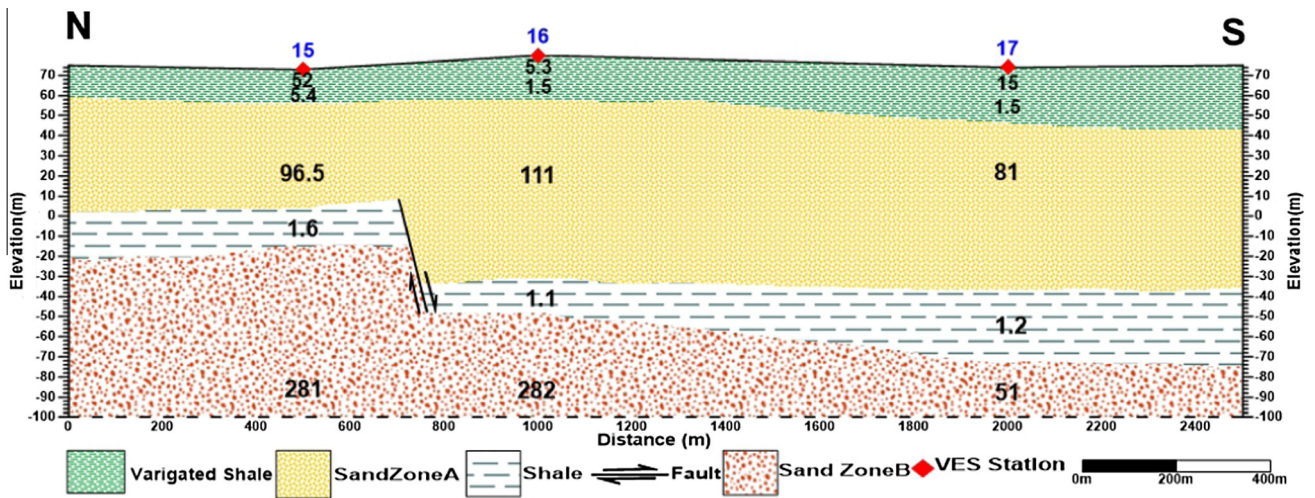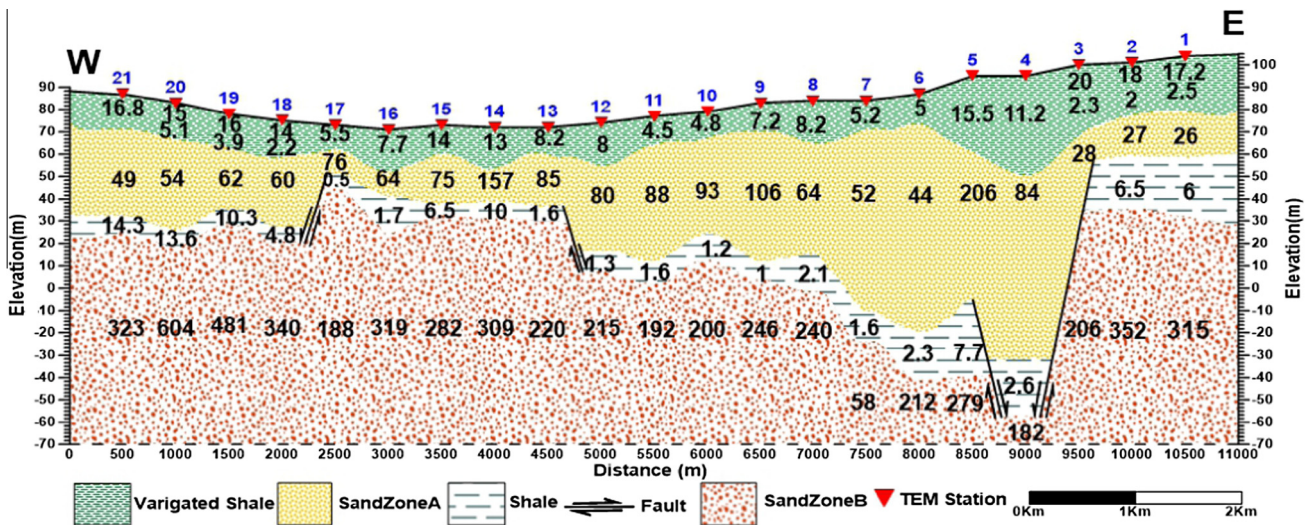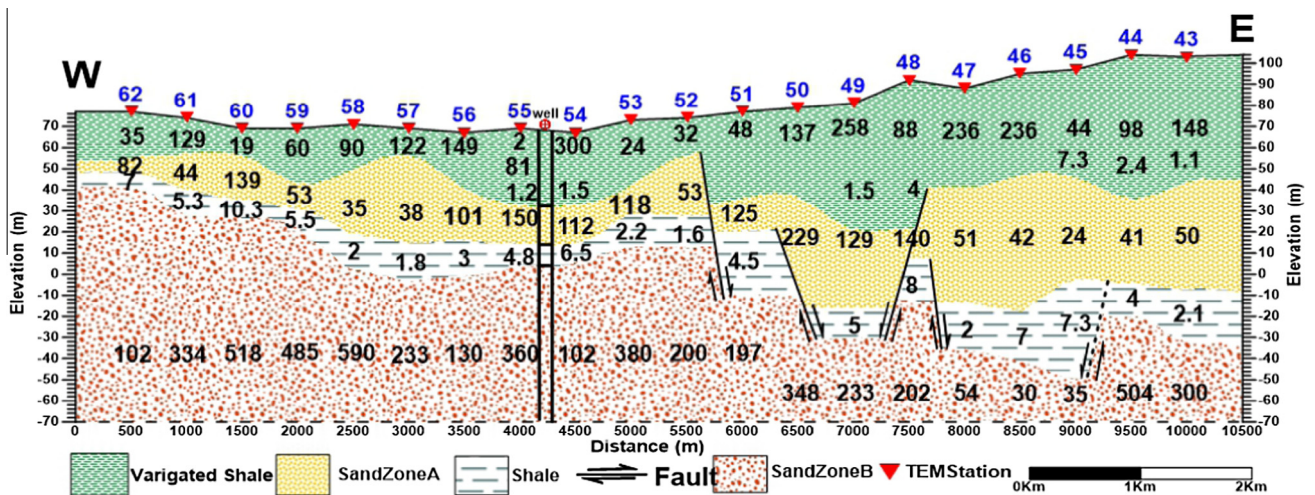

Figure 11   Geoelectrical/geological cross section constructed from TEM models along profile P3.
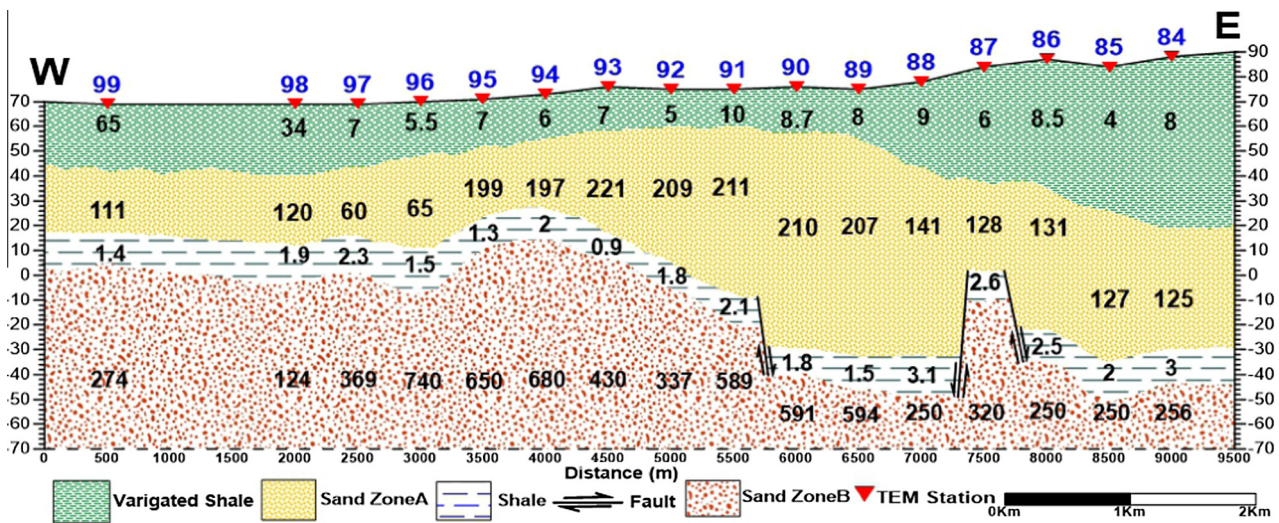
Figure 12 Geoelectrical/geological cross section constructed from TEM models along profile P5.
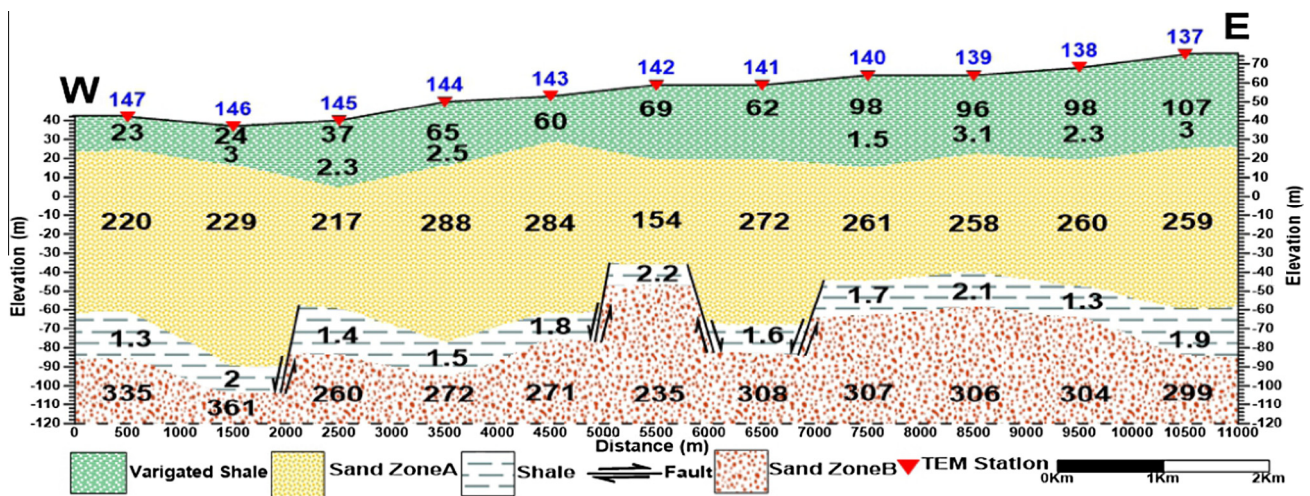

Figure 13 Geoelectrical/geological cross section constructed from TEM models along profile P9.

The TEM data were measured by SIROTEM *MK3* conductivity meter. The data were recorded at 167 points arranged along east–west trending lines with point–point spacing of 500–1000 m and line–line distance of about 2 km as shown in Fig. 5. The TEM data were acquired by using a single loop configuration with a loop-side length of 50, where the same loop was used for transmitting and receiving of EM signals.

5. Data analysis

5.1. VES data

The apparent resistivity values were plotted on a log–log paper. The obtained sounding curves show similar resistivity behavior across the studied area. This similarity in resistivity curves may indicate similar lithologic and/or hydrologic conditions of the studied area. The VES data were inverted in 1-D scheme by IPI2Win program and the final output is a set of multi-layer models each of them describes the geoelectrical parameters of subsurface layers at its respective site. Fig. 6

shows an example of the obtained models at sounding No. 6 correlated with the nearby borehole El-Sherka well No. 7. The model (blue line) exhibits a good matching with borehole information, and the model response (red curve) shows a best fitting with the measured data (black circles).

5.2. TEM data

The TEM data were recorded as a voltage response at a number of discrete time intervals. At each point, the data were recorded for several times and the logged data have been stacked to improve signal/noise ratio. Then, the data were normalized to the transmitter current and the best signal/noise ratio data set was selected to further processing and analysis (Soliman, 2005; Shaaban, 2009; Metwaly et al., 2010; Massoud et al., 2010; Younis, 2012).

TEMIX XL4 (2000) and IX1D (2007) programs were used for processing and inversion of TEM data. To determine the most robust models, the VES models were used as input models in TEM data inversion. Then, the trial -and -error approach was

(a)

(b)

(c)
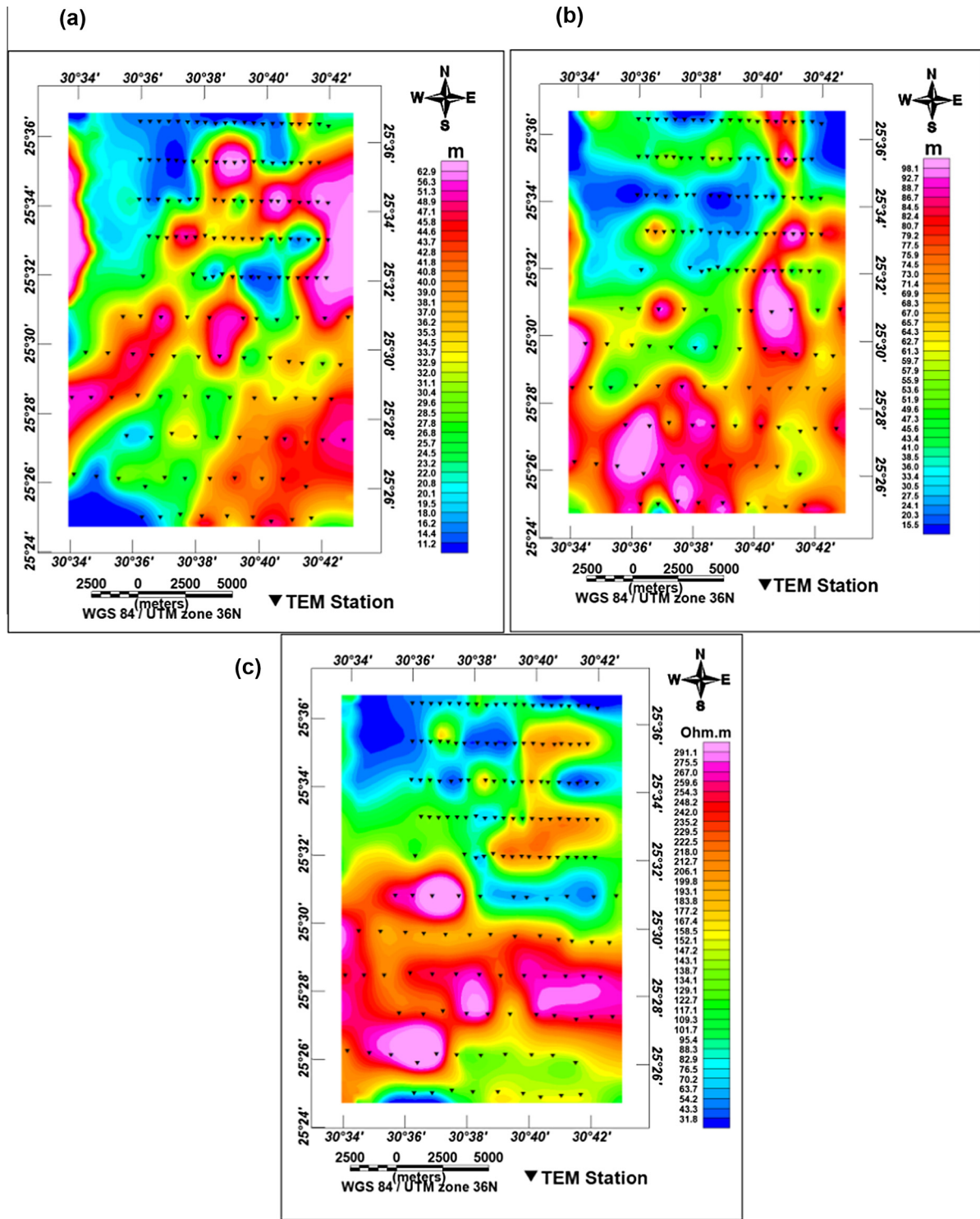
Figure 14 Contour maps describe the following: (a) depth to the upper surface, (b) thickness and (c) resistivity distribution in zone (A).

applied to the comparable data sets with fixing of some parameters to give a single model satisfies both data sets Besides, the available borehole data were used to control the inversion process of VES/TEM data. Fig. 7 shows an example of the TEM data inversion correlated with borehole information.

The final models obtained from TEM data inversion, constrained by VES models and geological information, were used for construction of geoelectrical/geological cross sections

describing the electrical parameters of subsurface medium in the study area.

6. Geoelectrical/geological sections

Based on the available geological information, the final multi-layer models have been utilized for construction of 6 cross sections by using the VES models and 11 cross sections by

Figure 15 Contour maps describe the following: (a) depth to the upper surface, and (b) resistivity distribution in zone (B).

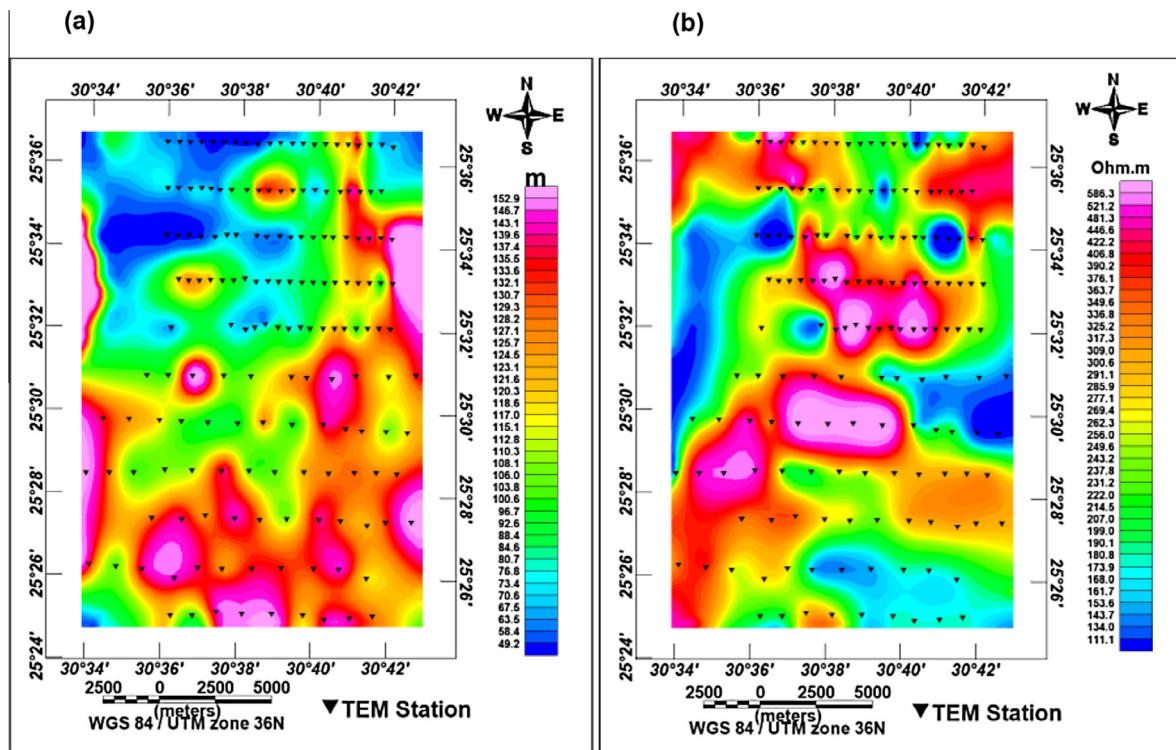using the TEM models. Locations and directions of these sections (profiles) are shown in Fig. 5. The VES sections were used for description of the vertical and lateral variation of resistivity in almost north–south direction, while the TEM sections were useful for describing the vertical and lateral variations in east–west direction. Examples of the constructed geoelectrical/geological cross sections are shown in Figs. 8–13.

As shown in the fore-mentioned sections, four geoelectric units could be identified in subsurface medium. These units seem to be extended in both north–south and east–west directions across the entire area. Besides, the VES sections show a good coherency with the TEM sections. The identified geoelectric units can be described in light of geological information as follows:

- The first (uppermost) unit exhibits a wide range of resistivity values ranging from 5 to more than 500 Ω m and a variable thickness ranging from 10 to 70 m. This unit could be correlated with the variegated shale deposits.
- The second unit exhibits low to moderate resistivity values ranging from 25 to 360 Ω m, thickness values ranging from 25 to 90 m and it was detected at 10–70 m depth below ground surface (bgs). This unit could be correlated with the shallowest zone (A) of the Nubian sandstone aquifer which is the main groundwater reservoir in the Western Desert including the study area. It is composed mainly of fine to medium sand intercalated with thin clay layers.
- The third unit is highly conductive with resistivity values ranging from 1.0 to 15 Ω m, thickness of 10–25 m and depth values of 35–150 m. This unit represents the green to black shale layer which splits the shallower zone (A) of the aquifer from the deeper zone (B).

- The fourth unit could be correlated with zone (B) of the Nubian sandstone aquifer in the study area. It shows resistivity values varying from 50 to 850 Ω m with depth values of 60–165 m bgs. The lower surface of zone (B) could not be detected by the applied acquisition parameters. This unit consists of medium to coarse sand with clay intercalations.

From structural viewpoint, several fault elements dissect the subsurface layers at the study area in both north–south and east–west directions. These faults control the groundwater flow and accumulation in the aquifer zones.

7. Water-bearing formations

Based on the applied data acquisition parameters and the obtained geophysical results, two zones (A and B) of the Nubian aquifer could be described.

7.1. Zone (A)

Zone (A) represents the first (uppermost) unit of the Nubian aquifer. It is composed of fine to medium sand with thin clay intercalations. Groundwater exists in this unit under unconfined to semi-confined conditions. As the TEM data provided a full coverage for the study area, the obtained TEM models were used for preparing 3 maps (Fig. 14a–c) describing the depth, thickness and resistivity distribution in this zone. As shown in Fig. 14, the unit (Zone A) exhibits resistivity values varying from 25 to 360 Ω m, thickness of 25–90 m and variable depth of 10–70 m to the upper surface of this unit. The low resistivity zones within this unit could be attributed to

existence of clay intercalations, and thinning of this unit at some locations could be attributed to the faulting effect. Integrated interpretation of the resistivity, thickness and depth maps indicates that groundwater can be obtained from this unit with relative priorities. The first priority (higher preference) can be given to the southwestern part of the unit which shows high resistivity (good water quality), high thickness (high water content) and low depth (low drilling cost).

7.2. Zone (B)

The second unit of the aquifer (zone B) comprises successive layers of medium to coarse sand, moderately sorted, with intercalations of clay. The upper surface of this unit could be detected at depth of 60–165 m bgs, and the unit shows resistivity values ranging from 50 to 850 Ω m (Fig. 15). The lower surface of this unit could not be reached. To obtain water from this unit, the first preference can be given to the central part of the study area.

8. Summary and conclusions

Geological, hydrogeologic and borehole information revealed that the Nubian sandstone aquifer is the main groundwater reservoir in Kharga basin including the study area. It comprises four sandy zones (A, B, C and D) separated from each other by shale layers. The aquifer is the sole source for water supplies in this area. However, it suffers from water table depletion due to over exploitation and un-managed withdrawal.

This study aimed at characterizing the present situation of groundwater in the shallow Nubian aquifer (zones A and B) at the northern part of Kharga basin. The lower Nubian aquifer (zones C and D) could not be studied in this stage due to the limited penetration depth of the applied geophysical techniques.

Inspection of the obtained geophysical results and correlation with the available geological, and hydrogeologic information revealed that the studied zones (A and B) are composed of successive layers of graded sand intercalated with thin clay layers. Both zones were affected by several fault elements striking in different directions and controlling groundwater flow and accumulation.

Resistivity distribution maps indicate that groundwater in the lower zone (B) might be of good quality than the water in zone (A). The most proper locations for drilling new water wells occupy the southwestern part of the study area for zone (A) and the central area for tapping zone (B).

Further geophysical studies are recommended by using other techniques with greater investigation depth (e.g. Magnetotellurics) to evaluate the lower Nubian aquifer (zones C and D).

Acknowledgments

References

Abd Allah, H.F., 2013. Environmental Impacts of over Exploitation on the Nubian Sandstone Aquifer in some localities, North EL-Kharga Oasis, Western desert, Egypt. M.Sc. Thesis, Menoufia University. Faculty of Science. Department of Geology. 127p.

Abdallah, K.A., 2000. Hydrogeological studies for re-evaluation of conditions and potentialities of the groundwater aquifer of El-Kharga Oasis Western desert – Egypt. M.Sc. Thesis, Faculty of Science, Cairo University, 200p.

Abu Seif, E.S., 2013. Performance of cement mortar made with fine aggregates of Dune Sand, Kharga Oasis, and Western Desert, Egypt: an experimental study. Jordan J. Civ. Eng. 7 (3), 270–284.

Beadnell, H.J.L., 1933. Remarks on the prehistoric geography and underground waters of Kharga Oasis. Geogr. J. 81 (2), 128–134.

CONOCO, 1987. Geological map of Egypt (scale 1:500,000).

Diab M.Sh., 1978. A regional hydrogeological study of artesian water aquifer in the Western Desert of Egypt: symposium on the geology of Middle East, Anqara, Turkey.

El-Hinnawi, M.H., Said, M.M., El-Kelani, A.H., Attya, M.N., 2005. Stratigraphic lexicon and exploratory notes to the geological map of the South Western Desert, Egypt. Joint Project between: EGSM, NARSS, UNDP and UNESCO. Publ. EGSMA, 117p.

El-Sankary, M.M., 2002. Geological, sedimentological and radioactivity studies of the quaternary sediments, El Kharga Depression, Western Desert, Egypt (Ph.D. thesis), Ain Shams Univ., Cairo, Egypt, 241p.

El-Shazly, M.M., Shata, A., Farag, L., 1959. Contribution to the study of the stratigraphy of El Kharga Oasis. Bull. de l'Inst. Du Desert d'Egypt 10 (1).

Ezzat, M.A., Abou El-Atta, A., 1974. Exploitation of groundwater in the Kharga Oasis, Part IV of the groundwater series in A.R.E., Ministry of Agriculture and Land Reclamation, Cairo.

Ghobrial, M.G., 1967. The structural geology of Kharga Oasis, Egypt Geol. Survey Paper No. 43, 39p.

IPI2WIN, 2011. Programs for resistivity and induced polarization sounding interpretation version 3.1.2c Bobachev A. A., programs set for VES data interpretation. Dep. of Geophysics, Geological Faculty, Moscow State University, Russia.

Issawi, B., El-Hinnawi, M.H., 1982. Kharga Oasis: A Case Study. Remote Sensing Center, Cairo, Egypt, p. 31p.

IX1D, 2007. IX1D V3 User's Manual. Interpex, Colorado, p. 133.

Knetsch, G., Yallouze, M., 1955. Remarks on the origin of the Egyptian oasis depressions. Bull. Soc. Geogr. Egypt 28, 21–33.

Massoud, U., Santos, F., El Qady, G., Attya, M., Soliman, S., 2010. Identification of the Shallow subsurface succession and investigation of the seawater invasion to the quaternary aquifer at the Northern part of El Qaa plain, Southern Sinai, Egypt by transient electromagnetic data. Geophys. Prospect. 58, 267–277.

Metwaly, M., El-Qady, G., Massoud, U., El-Kenawy, A., Matsushimi, J., 2010. Integrated geoelectrical survey for groundwater and shallow subsurface evaluation: case study at Siliyin spring, El-Fayoum, Egypt. Int. J. Earth Sci. 99, 1427–1436.

RIGW, 2006. Southern Egypt Development Project. Research Institute for Ground Water, unpublished internal report, 16p.

Rubin, Y., Hubbard, S.S., 2005. Hydrogeophysics. Springer, The Netherlands, p. 583p.

Said, R., 1962. The Geology of Egypt. Elsevier, Amsterdam-New York, p. 377p.

Said, R., 1990. The Geology of Egypt. In: Balkema, A.A. (ED.). Rotterdam-Brookfield, 734p.

Salman, A.B., 1984. Bibliography of geology and related sciences concerning Western Desert, Egypt, 1732–1984. Egyptian Geological Consulting Office "EGCO", Cairo, Egypt, 151p.

Salman, A.B., El-Aassy, I.E., El-Rakaiby, M.L., 1984. Contribution to radioactivity of South Western Desert, Egypt. Ann. Geol. Surv. Egypt 14, 43–57.

Salman, A.B., Howari, F.M., El-Sankary, M.M., Wali, A.M., Saleh, M.M., 2010. Environmental impact and natural hazards on Kharga Oasis monumental sites, Western Desert of Egypt. Afr. Earth Sci. 58, 341–353.

Shaaban, H.M., 2009. Applications of the geophysical survey for environmental and archeological purposes, central western part of the Nile Delta, EGYPT. M.Sc Thesis, Faculty of Science, Mansoura University, Egypt, 153p.

Shata, A., 1961. Remarks on the regional geologic structure of the groundwater reservoir of El Kharga and El Dakhla Oases. Bull. Soc. De Geogr. d'Egypt 34, 177–188.

Soliman, M.M., 2005. Environmental and geophysical assessment of the ground and subsurface water resources of Ras El-Hekma area, northwestern coast of Egypt. Ph.D. Thesis, Faculty of Science, Ain Shams University, Cairo, Egypt, 148p.

Soliman, S.M., 2013. Mitigation of excessive drawdowns via rotational groundwater withdrawal (Case study: El Kharga Oases, Egypt). N. Y. Sci. J. 6/1, 118–123.

Temix, X.L., 2000. TEMIX XL v4 User's Manual. Interpex, Colorado, USA, p. 468.

Vereecken, H., Yaramanci, U., Kemna, A., 2002. Non-invasive methods in hydrology Special issue. J. Hydrol. 267, 125–299.

Vereecken, H., Hubbard, S., Binley, A., Ferre, T., 2004. Hydrogeophysics. Introd. Guest Ed. Vadose Zone J. 3, 1060–1062.

Younis, A., 2012. Electromagnetic surveying methods for hydrocarbon exploration at the Nile Delta, Egypt. M.Sc. Thesis, Faculty of Science, Helwan University, Egypt, 143p.